Anisotropy of static and dynamic orientational correlations in *N*-alkanes

Ivet Bahar and Burak Erman
School of Engineering, Bogazici University, Bebek 80815, Istanbul, Turkey

(Received 15 June 1987; accepted 24 September 1987)

Static and dynamic orientational correlations in *n*-alkanes are analyzed using the rotational isomeric states formalism and its newly introduced adaptation to local chain dynamics. For systems in equilibrium, the anisotropy of directional correlations is investigated in relation to the respective orientations of two coordinate frames rigidly attached to the terminal bonds. The resulting static correlations exhibit a strong odd–even effect depending on the number of intervening bonds between the two frames. Dynamic correlations, on the other hand, necessitate the analysis of the time-dependent autocorrelation of a single reorienting frame rigidly embedded in the motional molecule. Expressions for both the *first* and *second* orientational correlation functions—identified according to the order of the associated Legendre polynomials—are formulated, for static and dynamic systems. Dynamic correlations are mathematically related to static correlations through the limiting values to which they asymptotically converge, as time goes to infinity. The orientational correlations are calculated to be strongly anisotropic in all cases.

I. INTRODUCTION

Statistical mechanical analysis of equilibrium configurations in *n*-alkanes and numerous other polymer chains of finite length reveals the highly asymmetric spatial distribution of atoms.[1,2] The density distribution $W(\mathbf{r})$ of the end-to-end vector $\mathbf{r}$ considerably departs from a symmetrical three-dimensional Gaussian distribution for chains with $N < 100$, where N denotes the number of skeletal bonds. The degree of anisotropy may be estimated by calculating the tensorial averages $\langle \mathbf{r}^{xp} \rangle$ of the pth direct product of the end-to-end vector.[1–3] Orientational correlations between two vectors affixed to two different locations along the chain are also indicative of the anisotropy intrinsic to polymeric structure. More specifically, correlations among the components of a vector affixed to a point along the chain with those of another vector at a different point give a complete description of anisotropy at equilibrium.

Consideration of the spatial anisotropy of configurations further suggests that dynamic transitions of specific directions from one state to the other should also be anisotropic. That the relaxation behavior for a vector rigidly embedded in the molecule depends on its specific orientation with respect to the main chain is confirmed by both previous theory and experiment.[4–7] The characterization of local motions stipulates, according to the theoretical analysis of Jarry and Monnerie,[7] the consideration of essentially two anisotropic quantities, referred to as (i) the orientation-mobility amplitude correlation describing how the amplitude of the motion is distributed among different initial orientations, and (ii) the directivity of mobility describing the relative intensity of motions in planes of different orientation. The orientational relaxation of various vectors rigidly attached to the polymer backbone was theoretically investigated by Weber and Helfand[6] through Brownian motion simulations. The decay of the autocorrelation functions with time was found to depend considerably on the direction of the investigated vector.[6] In fact, in fluorescence anisotropy decay experiments carried out by Valeur and Monnerie,[4] the fluorophore with its transition moment perpendicular to the backbone was found to relax much faster than that directed along a skeletal bond. Also, the discrepancy between the results from picosecond holographic technique and NMR measurements for a specific system, was attributed by Hyde *et al.*[5] to the fact that the reorientation of different intramolecular vectors were observed in the two experiments.

In the following section, we develop a mathematical method for calculating static and dynamic directional correlations in a chain. The application to real chains relies on the use of rotational isomeric states formalism, as presented in Sec. III. Also in the same section, dynamic correlations associated with conformational transitions of skeletal bonds are treated according to the recently introduced dynamic rotational isomeric state analysis.[8,9] The results from calculations are given in Sec. IV, which is followed by concluding remarks in Sec. V.

II. DEFINITIONS AND FORMULATION

Let A and B be two points along the polymer chain shown in Fig. 1. The vectors $\mathbf{a}_i$ at A and $\mathbf{b}_i$ at B represent two sets of orthonormal base vectors rigidly attached to the chain. Let $\mathbf{m}^A$ and $\mathbf{m}^B$ be two vectors rigidly embedded in the frames $\mathbf{a}_i$ and $\mathbf{b}_i$ at points A and B, respectively. They are written in component form as

$$\mathbf{m}^A = m_i^A \mathbf{a}_i, \quad \mathbf{m}^B = m_i^B \mathbf{b}_i, \tag{1}$$

where m_i^A and m_i^B are the scalar components of $\mathbf{m}^A$ and $\mathbf{m}^B$ along the frames $\mathbf{a}_i$ and $\mathbf{b}_i$, respectively. There is summation over repeated indices.

In order to analyze the internal correlations associated with configurational statistics we take the frame $\mathbf{a}_i$ as fixed and consider the static *cross-correlations* between the base vectors $\mathbf{a}_i$ and $\mathbf{b}_i$. Dynamic correlations, on the other hand, are determined by the time-dependent *autocorrelations* of the base vectors $\mathbf{b}_i(t)$ at time t.

 0021-9606/88/021228-07$02.10

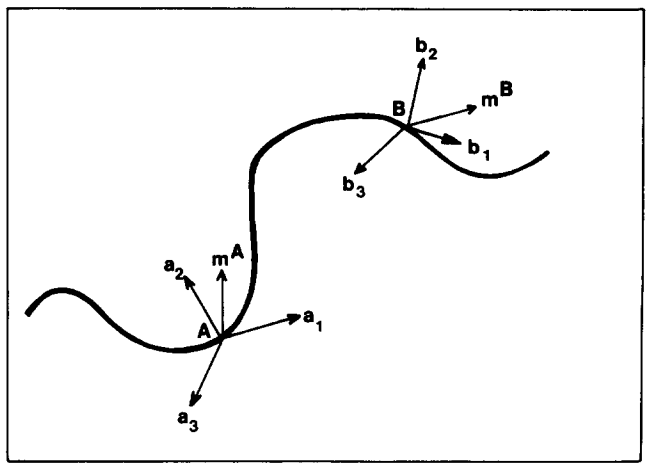

FIG. 1. Schematic representation of a portion of a short chain with two coordinate systems located at points A and B. The vectors $\mathbf{a}_i$ and $\mathbf{b}_i$ represent two sets of orthonormal base vectors attached at A and B, respectively. The vectors $\mathbf{m}^A$ and $\mathbf{m}^B$ are rigidly embedded in the two reference frames.

In general, experimental data are interpreted in terms of correlation functions employing first and second Legendre polynomials. First-order Legendre polynomials are involved in experiments such as dielectric relaxations, infrared absorption, etc.[10] while a broad class of experiments for probing molecular dynamics (dynamic light scattering, ESR, NMR, depolarization of fluorescence, etc.) are described by the Legendre polynomials of second order. In order to account for both types of experiments, first and second correlation functions in their most general anisotropic form will be defined in the following. They are classified into two groups, static and dynamic, comprising both the first and second correlation functions, separately.

A. Static correlations

We define the first static correlation function $S_{1,ij}$ as

$$S_{1,ij} \equiv \langle \mathbf{a}_i \cdot \mathbf{b}_j(0) \rangle. \tag{2}$$

Here the time argument of $\mathbf{a}_i$ is omitted as they are fixed in space. The dot denotes the scalar product.

The components of $\mathbf{b}_j$ may be represented with respect to the system $\mathbf{a}_i$ as

$$\mathbf{b}_j(t) = b_{ij}(t)\mathbf{a}_i, \tag{3}$$

where b_{ij} is the cosine of the angle between $\mathbf{a}_i$ and $\mathbf{b}_j$. Substituting Eq. (3) into Eq. (2) leads to

$$S_{1,ij} = \langle b_{ij}(0) \rangle. \tag{4}$$

Similarly, the second static correlation function may be defined as the fourth-rank tensor

$$S^{kl}_{2,ij} = \tfrac{1}{2}\langle 3[\mathbf{b}_i(0)\cdot\mathbf{a}_k][\mathbf{b}_j(0)\cdot\mathbf{a}_l] - \delta_{ij}\delta_{kl} \rangle, \tag{5}$$

where δ_{ij} is the Kronecker delta. Substituting from Eq. (3) into Eq. (5) gives

$$S^{kl}_{2,ij} = \tfrac{1}{2}\langle 3b_{ki}(0)b_{lj}(0) - \delta_{ij}\delta_{kl} \rangle \tag{6}$$

which is identical to the generalized order parameter tensor previously introduced for the analysis of liquid crystal systems.[11] $S^{kl}_{2,ij}$ is symmetric in the indices (i,j) and (k,l) separately and is traceless with respect to both pairs of indices, i.e., $S^{kl}_{2,ii} = S^{kk}_{2,ij} = 0$. This follows from the orthonormality of the reference frames $\mathbf{a}_i$ and $\mathbf{b}_j$, which may be expressed by the relation

$$b_{ij}(t)b_{ik}(t) = \delta_{jk}. \tag{7}$$

B. Dynamic correlation functions

For a stationary process, we define the first dynamic correlation function as

$$M_{1,ij}(t) = \langle \mathbf{b}_i(0)\cdot\mathbf{b}_j(t) \rangle \tag{8}$$

which may be represented through the use of Eq. (3) as

$$M_{1,ij}(t) = \langle b_{ki}(0)b_{kj}(t) \rangle. \tag{9}$$

At $t = 0$, the orthonormality condition leads to

$$M_{1,ij}(0) = \delta_{ij} \tag{10}$$

and at $t = \infty$, we have

$$M_{1,ij}(\infty) = \langle b_{ki}(0) \rangle \langle b_{kj}(0) \rangle = S_{1,ki}S_{1,kj}. \tag{11}$$

The second dynamic correlation function is defined as

$$M^{kl}_{2,ij}(t) = \tfrac{1}{2}\langle 3[\mathbf{b}_i(t)\cdot\mathbf{b}_k(0)][\mathbf{b}_j(t)\cdot\mathbf{b}_l(0)] - \delta_{ij}\delta_{kl} \rangle. \tag{12}$$

Substituting from Eq. (3) into Eq. (12), we obtain

$$M^{kl}_{2,ij}(t) = \tfrac{1}{2}\langle 3b_{mi}(t)b_{mk}(0)b_{nj}(0)b_{nl}(0) - \delta_{ij}\delta_{kl} \rangle. \tag{13}$$

At $t = 0$, Eq. (12) gives

$$M^{kl}_{2,ij}(0) = \tfrac{1}{2}(3\delta_{ik}\delta_{jl} - \delta_{ij}\delta_{kl}). \tag{14}$$

At $t = \infty$, Eq. (13) may be written as

$$\begin{aligned} M^{kl}_{2,ij}(\infty) &= \tfrac{3}{2}\langle b_{mi}(0)b_{nj}(0) \rangle \langle b_{mk}(0)b_{nl}(0) \rangle - \delta_{ij}\delta_{kl}/2 \\ &= \tfrac{2}{3} S^{mn}_{2,ij} S^{mn}_{2,kl}, \end{aligned} \tag{15}$$

where the second line is obtained by the use of Eq. (6).

III. ROTATIONAL ISOMERIC STATE CALCULATIONS OF CORRELATIONS

A. Static correlations

The all-*trans* configuration of an n-alkane chain of n repeating units is shown in Fig. 2. The reference frames $\mathbf{a}_i$ and $\mathbf{b}_i$ are affixed to the terminal bonds of the chain. Bond numbers are denoted on each bond. Φ_i is the torsional angle corresponding to bond i. For n-alkanes three isomeric states, *trans* (t), *gauche* $+$ (g^+), and *gauche* $-$ (g^-), characterized by $\Phi_i = 0°$, $+120°$, and $-120°$, respectively, are energetically most favorable. θ is the supplemental bond angle, assumed to be 68° for all consecutive bond pairs. The frame $\mathbf{a}_i$ is fixed in space as stated above. The first two bonds lie in the $\mathbf{a}_1 - \mathbf{a}_2$ plane. The transformation matrix from bond $i+1$ to bond i is

$$\mathbf{T}_i = \begin{bmatrix} \cos\theta & \sin\theta & 0 \\ \sin\theta\cos\Phi_i & -\cos\theta\cos\Phi_i & \sin\Phi_i \\ \sin\theta\sin\Phi_i & -\cos\theta\sin\Phi_i & -\cos\Phi_i \end{bmatrix}. \tag{16}$$

The equilibrium average $\langle b_{ij}(0) \rangle$ in Eq. (4) may conveniently be expressed in matrix notation as the ijth element of the first static correlation matrix $\langle \mathbf{S}_1 \rangle$. The latter is obtainable from the product of transformation matrices as

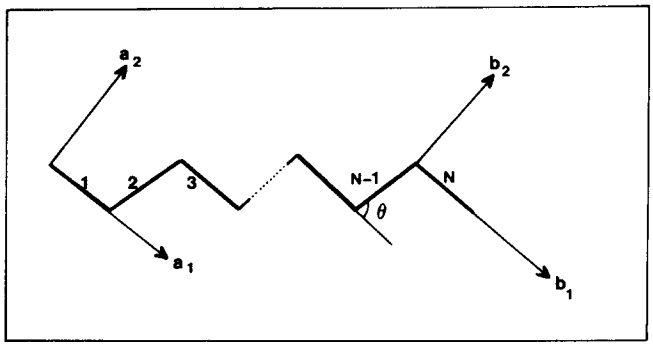

FIG. 2. Schematic representation of the all *trans* configuration of an *n*-alkane chain with *N* skeletal bonds. The frames $\mathbf{a}_i$ and $\mathbf{b}_i$ are affixed at both ends as described in the text. θ is the supplemental bond angle. The frame $\mathbf{a}_i$ is fixed in space while $\mathbf{b}_i$ undergoes translational and/or rotational motion depending on the internal configurational transitions of the chain.

$$\langle \mathbf{S}_1 \rangle = \langle \mathbf{T}_1\mathbf{T}_2\mathbf{T}_3\cdots\mathbf{T}_{n-1}\rangle. \tag{17}$$

The ensemble average in Eq. (17) is computed, according to the conventional rotational isomeric states formalism[1,9] from

$$\langle \mathbf{S}_1 \rangle = Z^{-1}(\mathbf{J}^*\otimes\mathbf{I}_3)\|\mathbf{T}_1\|\prod_{k=2}^{n-1}[(\mathbf{U}_k\otimes\mathbf{I}_3)\|\mathbf{T}_k\|](\mathbf{J}\otimes\mathbf{I}_3), \tag{18}$$

where $\otimes$ denotes the tensor product, k is the bond number index, and

$$Z = \mathbf{J}^*\mathbf{U}_2\left(\prod_{k=2}^{n-1}\mathbf{U}_k\right)\mathbf{U}_{n-1}\mathbf{J},$$

$$\mathbf{J}^* = [1\ \ 0\ \ 0],\quad \mathbf{J} = \begin{bmatrix}1\\1\\1\end{bmatrix},\quad \mathbf{I}_3 = \begin{bmatrix}1&0&0\\0&1&0\\0&0&1\end{bmatrix},$$

$$\mathbf{U}_k = \begin{bmatrix}1&\sigma&\sigma\\1&\sigma&\sigma\omega\\1&\sigma\omega&\sigma\end{bmatrix},\quad 2<k<n-1, \tag{19}$$

$$\mathbf{U}_2 = \mathbf{U}_{n-1} = \begin{bmatrix}1&1&1\\1&1&0\\1&0&1\end{bmatrix},$$

$$\|\mathbf{T}\| = \begin{bmatrix}\mathbf{T}(\Phi=0^\circ)&&\\&\mathbf{T}(\Phi=120^\circ)&\\&&\mathbf{T}(\Phi=240^\circ)\end{bmatrix},$$

and

$$\sigma = \exp(-E_\sigma/RT),\quad \omega = \exp(-E_\omega/RT),$$

E_σ being the energy of a *gauche* state relative to *trans*, and E_ω that for a $g^\pm g^\mp$ pair in excess of the energy $2E_\sigma$. More detailed discussion of equilibrium statistics of *n*-alkanes and the matrix multiplication technique to generate configurational averages may be found elsewhere.[1,8,12]

It should be noted that the summation convention adopted throughout Sec. II is valid only for indices referring to coordinates and does not hold for those, in Sec. III, referring to bond sequence number and/or configuration number.

In analogy with the above treatment the average $\langle b_{ki}(0)b_{lj}(0)\rangle$ [in Eq. (6)] involving four indices may be associated with a fourth-rank tensor $\langle S_2\rangle$, referred to as the second static correlation tensor. The latter will be given by

$$\langle \mathbf{S}_2 \rangle = \tfrac{1}{2}(3\langle \mathbf{S}_1\otimes\mathbf{S}_1\rangle - \mathbf{I}_9), \tag{20}$$

where the quantity $\langle b_{ki}(0)b_{lj}(0)\rangle$ has been replaced by

$$\langle(\mathbf{T}_1\mathbf{T}_2\cdots\mathbf{T}_{n-1})\otimes(\mathbf{T}_1\mathbf{T}_2\cdots\mathbf{T}_{n-1})\rangle = \langle \mathbf{S}_1\otimes\mathbf{S}_1\rangle$$

and $\mathbf{I}_9$ is the identity matrix of order 9. The term $\langle \mathbf{S}_1\otimes\mathbf{S}_1\rangle$ is readily evaluated from

$$\langle \mathbf{S}_1\otimes\mathbf{S}_1\rangle = \left\langle\prod_{i=1}^{n-1}(\mathbf{T}_i\otimes\mathbf{T}_i)\right\rangle$$
$$= Z^{-1}(\mathbf{J}^*\otimes\mathbf{I}_9)\|\mathbf{T}_1\otimes\mathbf{T}_1\|$$
$$\times\prod_{k=2}^{n-1}[\mathbf{U}_k\otimes\mathbf{I}_9\|\mathbf{T}_k\otimes\mathbf{T}_k\|]\mathbf{J}\otimes\mathbf{I}_9, \tag{21}$$

where the first equality results from the theorem on direct products.

B. Dynamic correlations

The stochastics of conformational transitions of N sequential bonds is fully described by the time-dependent joint probability matrix $\mathscr{P}^{(N)}(t)$ (Ref. 9). 3^N configurations denoted each by $\{\Phi\}_i$, $i = 1$ to 3^N, are available to an N-bond sequence on the basis of three isomeric states per bond. The ijth element $\mathscr{P}_{ij}^{(N)}(t)$ of $\mathscr{P}^{(N)}(t)$ represents the joint probability of occurrence of the configuration $\{\Phi\}_i$ at time t and $\{\Phi\}_j$ at $t=0$. Let us consider, for example, the element $\mathscr{P}_{ij}^{(N)}(t)$ for the passage to state $\{\Phi\}_j = \{\alpha\beta\gamma\delta\cdots\}$ at time t, from the initial state $\{\Phi\}_i = \{\alpha'\beta'\gamma'\delta'\cdots\}$. This element will be represented by the symbol $p(\alpha\beta\gamma\delta,...,t;\alpha'\beta'\gamma'\delta',...,0)$. Here $\alpha,\beta,\gamma,\delta$,etc. denote the isomeric states of successive skeletal bonds. As in the treatment of equilibrium statistics the interdependence of skeletal bonds is incorporated in the theory, through adoption of pairwise dependent transitions.[9] Thus,

$$p(\alpha\beta\gamma\delta,...,t;\alpha'\beta'\gamma'\delta',...,0)$$
$$= p(\alpha\beta,t;\alpha'\beta',0)q(\beta\gamma,t;\beta'\gamma',0)q(\gamma\delta,t;\gamma'\delta',0), \tag{22}$$

where

$$q(\beta\gamma,t;\beta'\gamma',0)$$
$$= p(\beta\gamma,t;\beta'\gamma',0)/\sum_n\sum_\zeta p(\beta\eta,t;\beta'\zeta,0). \tag{23}$$

The summation in Eq. (23) is over all possible rotational states, thus includes nine terms for $\eta = t,g^+,g^-$ and $\zeta = t,g^+,g^-$. The term $q(\beta\gamma,t;\beta'\gamma',0)$ gives the conditional probability of transition from initial state γ' to state γ at time t for the second bond of a pair, given that the first bond undergoes the transition from state β' to β. The problem thus reduces to the evaluation of joint probabilities for the pairs such as $p(\alpha\beta,t;\alpha'\beta',0)$, i.e., the elements of $\mathscr{P}^{(2)}(t)$. $\mathscr{P}^{(2)}(t)$ are evaluated from[8,9]

$$\mathscr{P}^{(2)}(t) = \exp\{\mathbf{A}^{(2)}(t)\}\mathscr{P}^{(2)}(0)$$
$$= \mathbf{B}^{(2)}\exp\{\mathbf{L}^{(2)}(t)\}[\mathbf{B}^{(2)}]^{-1}\,\mathrm{diag}\,\mathscr{P}^{(2)}(0), \tag{24}$$

where $\mathbf{B}^{(2)}$ is the matrix formed from the eigenvectors of $\mathbf{A}^{(2)}$, $\mathbf{L}^{(2)}$ the diagonal matrix of the eigenvalues of $\mathbf{A}^{(2)}$. $\mathbf{A}^{(2)}$ is the

9×9 matrix whose ijth element describes the momentary rate of passage from initial configuration $\{\Phi\}_j$ to $\{\Phi\}_i$ at time t. Kramer's high friction rate expression,[13] also adopted by Helfand and Skolnick[14] in their kinetic treatment of conformational transitions is used in the elements of $\mathbf{A}^{(2)}$. The activation energies in the rate expressions are determined from the heights of saddles between isomeric states, on the basis of two-dimensional energy maps.[9]

Pursuant to the calculation of first and second dynamic correlation functions, the elements $\mathscr{P}_{ij}^{(N)}(t)$ are used as stochastic weights for the passage from configuration $\{\Phi\}_j$ to configuration $\{\Phi\}_i$. Consequently, the second-rank tensor $\mathbf{M}_1(t)$ of the first dynamic correlation functions becomes

$$\mathbf{M}_1(t)=\sum_i\sum_j[\mathscr{P}_{ij}^{(N)}(t)\mathbf{F}_i^T\mathbf{F}_j], \tag{25}$$

where $\mathbf{F}_i\equiv(\mathbf{T}_1\mathbf{T}_2\cdots\mathbf{T}_{n-1})_i$ is the product of transformation matrices for configuration $\{\Phi\}_i$ and $\mathbf{F}_i^T$ is its transpose.

Similarly, the second dynamic correlation tensor $\mathbf{M}_2(t)$ is obtained from

$$\mathbf{M}_2(t)=\frac{1}{2}\left[3\sum_i\sum_j\mathscr{P}_{ij}^{(N)}(t)\mathbf{G}_i^T\mathbf{G}_j-\mathbf{I}_9\right], \tag{26}$$

where

$$\mathbf{G}_i\equiv\mathbf{F}_i\otimes\mathbf{F}_i=\left[\prod_{k=1}^{n-1}(\mathbf{T}_k\otimes\mathbf{T}_k)\right]_i \tag{27}$$

is characteristic of a specific configuration $\{\Phi\}_i$.

IV. CALCULATIONS

Calculations were performed for n-alkanes, C_nH_{2n+2}, with n varying from 6 to 11. The terminal bonds being kept in *trans* state, 3^{N-2} configurations, where $N=n-1$ is the number of skeletal bonds, are available for C_nH_{2n+2}. The energies $E_\sigma=0.5$ and $E_\omega=2.2$ kcal/mol were used at $T=300$ K. Both static and dynamic correlations were considered and will be presented separately.

A. Static correlations

First and second static correlation tensors are calculated from Eq. (17) and Eqs. (20) and (21), respectively. The results from calculations are given in Figs. 3 and 4, as a function of chain length represented by the number of skeletal bonds N. Both figures display the strong odd–even effect, characteristic of short chains, which is expected to gradually disappear with increasing chain length. In Fig. 3 the three principal values (11, 22, and 33) of the tensor $\langle\mathbf{S}_1\rangle$ are shown by the solid broken lines. The dashed line represents the 12 (or 21) component, the only nonzero cross-correlation function in $\langle\mathbf{S}_1\rangle$. A larger number of correlation functions is involved in the second static correlation tensor $\langle\mathbf{S}_2\rangle$. However the number of distinct correlation functions is considerably reduced due to symmetry relationships ($S_{2,ij}^{kl}=S_{2,ji}^{kl}$ and $S_{2,ij}^{kl}=S_{2,kl}^{ij}$) and orthonormality conditions ($S_{2,ii}^{kl}=1$). Let us consider the nine correlation functions $S_{2,ii}^{jj}$ (In the following, there is no summation over repeated indices. In the figures, underscores are placed under the indices to suspend summation.) Six equations resulting from the interchangeability of upper and lower indices and from orthonormality conditions reduce the number of

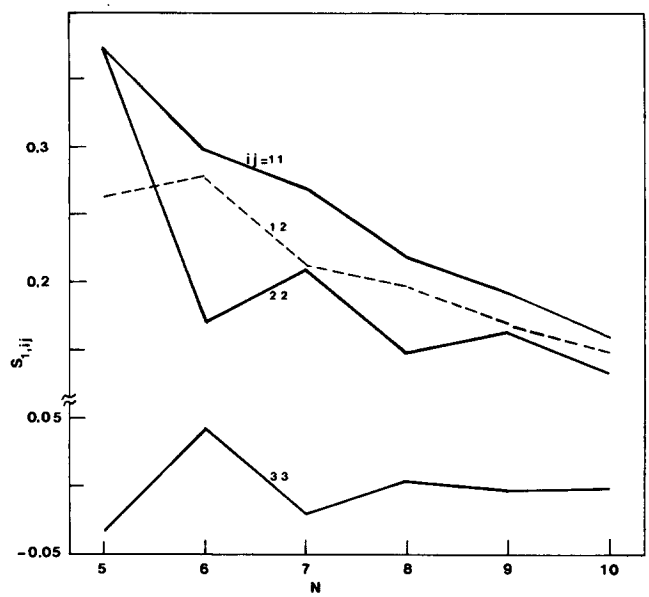

FIG. 3. Dependence of the *first* static orientational correlation function on chain length. The three principal values $S_{1,ii}$ of the tensor $\langle\mathbf{S}_1\rangle$ are shown by the solid lines as a function of the number N of skeletal bond. The only nonvanishing cross-correlation $S_{1,12}$ is shown by the dashed line. Curves in Figs. 3–8 are calculated for $T=300$ K, $E_\sigma=0.5$, and $E_\omega=2.2$ kcal/mol.

independent unknowns to three. Thus, specification of the three correlation functions $S_{2,ii}^{ii}$ with $i=1,2,3$ fixes the remaining six functions. Consequently, only the relevant correlation functions $S_{2,ii}^{ii}$ ($i=1,2,3$) are shown in Fig. 4. As to the remaining correlation functions $S_{2,ij}^{kl}$ with $i\neq j$ and/or $k\neq l$, they are not reported in the present study inasmuch as no current experimental data are available for their verification. It should be mentioned, however, that all $S_{2,ij}^{kl}$ where one of the indices equals three are identically equal to zero, due to the symmetry of the chain structure with respect to

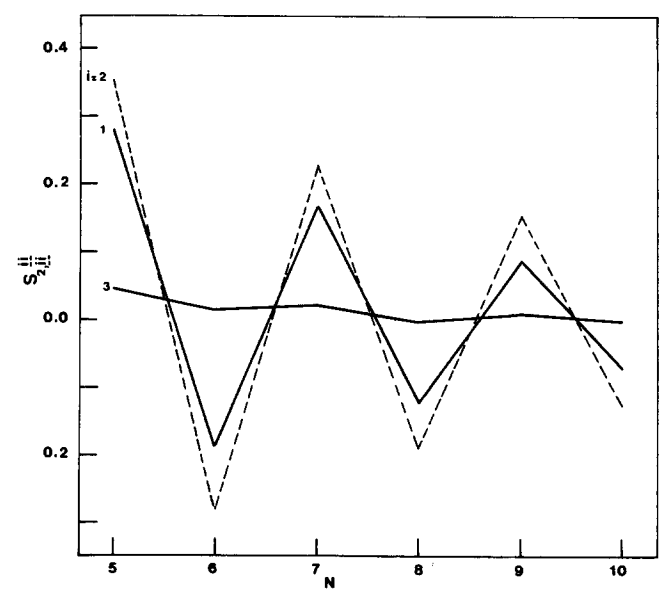

FIG. 4. Dependence of the *second* static orientational correlation function on chain length. The three components $S_{2,ii}^{ii}$ ($i=1,2,3$) of the tensor $\langle\mathbf{S}_2\rangle$ are calculated for various N. The result for $i=2$ is shown by the dashed line for clarity.

the $\mathbf{a}_1\mathbf{a}_2$ plane. The remaining functions are symmetric in the indices (i,j) and (k,l), as expected.

The analysis of Figs. 3 and 4 reveals the highly anisotropic character of static correlations in finite chains.

B. Dynamic correlations

The calculation of dynamic correlation functions necessitates the analysis of pairwise dependent conformational transitions. To this end, the matrix $\mathbf{A}^{(2)}$ for n-alkanes, as given explicity in Ref. 9, was used in Eq. (24). The obtained joint probabilities for the pairs were in turn substituted into Eqs. (22) and (23) to determine $\mathscr{P}^{(N)}(t)$. The elements of the latter are used in Eqs. (25) and (26) to compute the first and second dynamic correlation tensors, respectively.

By repeating the calculation scheme described above for various times, the relaxation curves depicted in Figs. 5 and 6 are obtained. The curves are drawn for $N = 6$ and $T = 300$ K. Figure 5 displays the decay of the principal values $M_{1,ii}$ $(i = 1,2,3)$ of the first dynamic correlation tensor $\mathbf{M}_1(t)$, while the curves in Fig. 6 exhibit the decay of the three autocorrelation functions $\mathbf{M}^{ii}_{2,ii}$ $(i = 1,2,3)$ of the second dynamic correlation tensor $\mathbf{M}_2(t)$. In both cases, the vector perpendicular to the backbone $(i = 3)$ relaxes most rapidly and to the lowest asymptotic value. The relative behavior of the correlation functions with $i = 1$ and 2 depends on the type (first or second) of the orientational correlation investigated. In both figures the correlation functions for $N = 8$ and $i = 3$ are shown by the lowest dashed line. Faster relaxation with longer sequences is indicative of the higher number of paths available for relaxation. This behavior, however, is expected to be eventually reversed, as the sequence size increases, owing to gradually dominating frictional resistance.

The limiting values to which the dynamic correlation functions asymptotically converge as t goes to infinity are shown in Figs. 7 and 8, for various chain lengths. The curves are obtained using Eq. (11) for $\mathbf{M}_1(\infty)$ and Eq. (15) for $\mathbf{M}_2(\infty)$. It is seen that the unit vector in the z direction (i.e.,

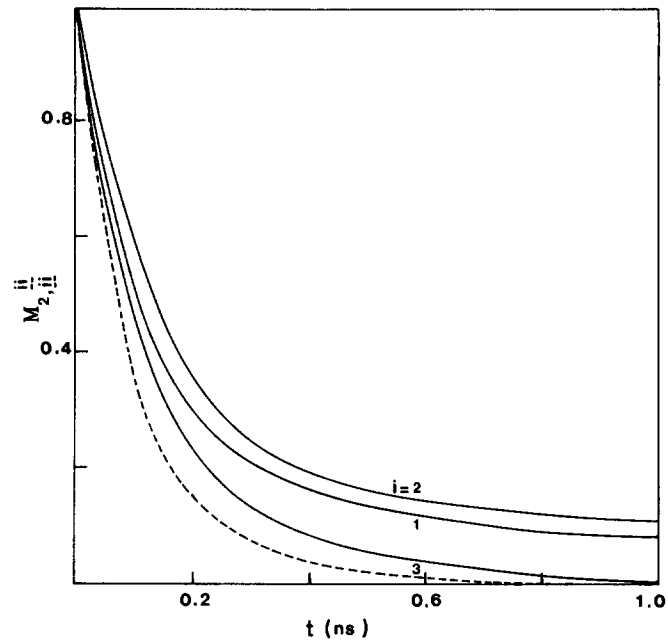

FIG. 6. Time dependence of the *second* dynamic correlation tensor $\mathbf{M}_2$. The decay of the three values $M^{ii}_{2,ii}$ with $i = 1,2,3$ for $N = 6$ are shown by the solid curves. The decay for $i = 2$ is calculated to be slower than that for $i = 1$, in contrast to the results for the *first* dynamic correlation tensor shown in Fig. 5. The dashed curve is calculated for $i = 3$, $N = 8$.

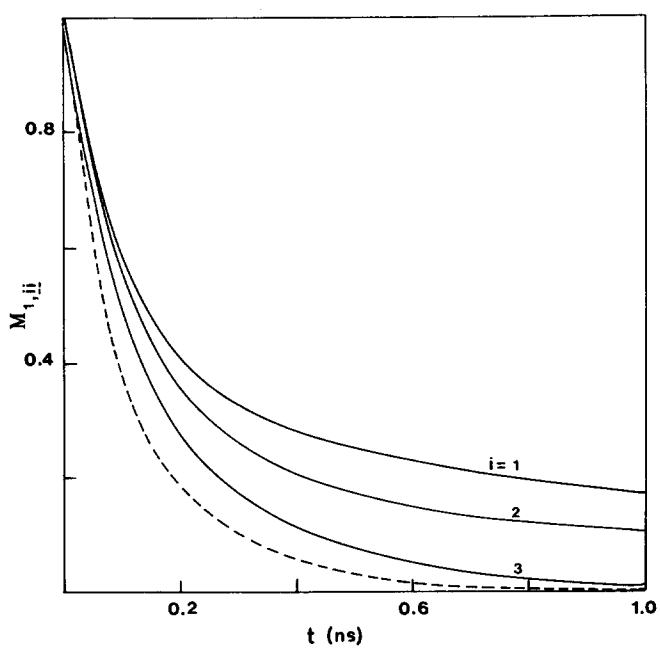

FIG. 5. Principal values $M_{1,ii}$ of the *first* dynamic orientational correlation tensor $\mathbf{M}_1$ vs time (t in nanoseconds) for $N = 6$. The dashed curve represents $M_{1,33}(t)$ for $N = 8$.

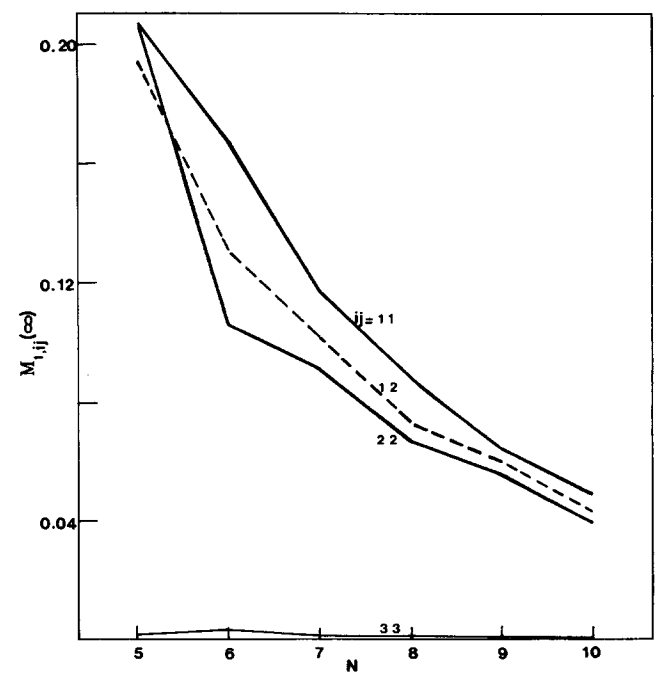

FIG. 7. $M_{1,ii}(\infty)$ vs N, for $i = 1,2,3$. The argument of $M_{1,ii}$ indicates the ultimate values to which the correlation functions asymptotically converge in the limit as $t \to \infty$. The result for $M_{1,12}$ is given by the dashed curve.

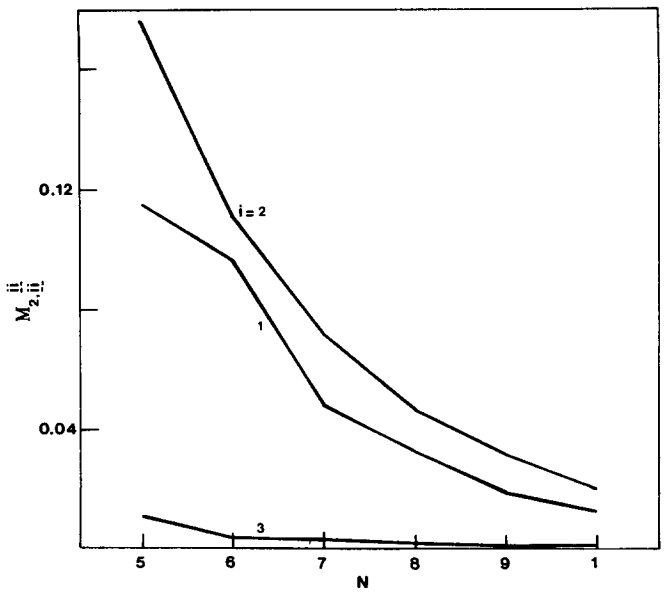

FIG. 8. $M^{ii}_{2,ii}(\infty)$ vs N, for $i = 1,2,3$. Figures 7 and 8 show that for short chains ($N < 10$) some internal orientational autocorrelation inherently resulting from chain structure and equilibrium statistics, persists, for the motional frame $\mathbf{b}_i$, regardless of the time domain.

$\mathbf{b}_3$) of the bond-based reference frames is almost uncorrelated regardless of the chain length. However, a finite autocorrelation indefinitely persists for the remaining two components of the reorientating frame, for $N < 10$, as concluded from the nonzero dynamic autocorrelation functions for $t = \infty$ in both figures. The vector $\mathbf{b}_1$ exhibits stronger autocorrelation compared to $\mathbf{b}_2$ in Fig. 7 while the opposite situation occurs in Fig. 8. The change in their relative magnitudes is consistent with the preceding calculations (Figs. 3–6).

V. CONCLUSION

In the present work, static and dynamic correlations in *n*-alkanes were considered in relation to the orientation of the investigated vector with respect to the main chain. Static correlations were computed on the basis of conventional rotational isomeric states formalism and the related matrix multiplication techniques. Dynamic correlations were investigated using a recently introduced approach where the structural properties of *n*-alkanes are incorporated into the calculation scheme through the use of the rate matrix $\mathbf{A}^{(2)}$ describing the momentary rate of passage over saddles in energy maps.

Both static and dynamic correlations are classified into two groups referred to as the first and second correlation functions. Such a classification was necessary in view of the fact that different correlation functions are probed in various experiments. For instance, Fourier transforms of *first* static and dynamic correlations resulting from the collective contribution of a group of permanent dipoles is observed in dielectric relaxation while most of spectroscopic experiments involve *second* correlation functions generally associated with the reorientation of a single vector. Previous theoretical models[15–19] of chain dynamics were found to fit the decay curves of both types of correlation functions by suitable adjustment of parameters. Thus as Skolnick and Yaris pointed out,[20] the model of Valeur, Jarry, Gény, and Monnerie,[15] the cutoff diffusion model of Bendler and Yaris,[16] the damped-diffusion model of Skolnick and Yaris, all predict the equivalence of the two types of dynamic correlation functions. From the examination of Figs. 5–8, it is seen that the principal values of the two tensors $\mathbf{M}_1(t)$ and $\mathbf{M}_2(t)$ exhibit similar dependence on time and converge asymptotically to about the same limiting values. Thus, although *second* dynamic correlations relax slightly faster and to somewhat lower limiting values compared to those associated with $\mathbf{M}_1(t)$, same functional forms may, in fact, represent, as a first approximation, both types of correlation functions by suitable choice of parameters. However a clear distinction between them appears on the grounds of their anisotropic character. Vectors along the main chain ($\mathbf{b}_1$) exhibit strongest autocorrelation as far as *first* dynamic correlations are concerned but as to the *second* dynamic correlations, the relative behavior of $\mathbf{b}_1$ and $\mathbf{b}_2$ is inverted. $\mathbf{b}_2$ relaxes more slowly and to higher asympotic value. This feature draws attention to the importance of the relative orientation of the investigated vector (e.g., the transition moments of chromophores, the ^{13}C–H bonds) with respect to the main chain. The vector $\mathbf{b}_3$ relaxes very fast in both cases, in agreement with the out-of-plane vector in Weber and Helfand's simulations.[6]

From Figs. 2 and 3 it may be seen that static correlations possess the same type of anisotropy, as the dynamic ones. The odd–even effect in $\langle \mathbf{S}_2 \rangle$ is more pronounced compared to $\langle \mathbf{S}_1 \rangle$. Again no significant correlation exists between vectors in z direction of bond-based reference frames. Persistence of directional correlation between the terminal bond vectors of α, ω disubstituted *n*-alkanes was theoretically and experimentally analyzed by Abe *et al.*[20] For $N \leqslant 10$ the directional correlation between the terminal bond vectors was found to be far from random.

Although the results are presented here for finite chains with one end fixed, they may also be adopted to the analysis of correlations in segments of long chains as previously treated.[9]

Another example of a sequence with a fixed end is encountered in the packing of short chain molecules in interphases such as bilayer membranes.[21] The organization of short chains in planar bilayers or in micelles or vesicles[22] is similar to that between crystalline and amorphous regions in lamellar semicrystalline polymers.[23] In all cases, the packing is expected to be strongly affected by the orientational anisotropy intrinsic to the polymeric structure.

[1] P. J. Flory, *Statistical Mechanics of Chain Molecules* (Interscience, New York, 1969).
[2] (a) P. J. Flory and D. Y. Yoon, J. Chem. Phys. **61**, 5358 (1974); (b) D. Y. Yoon and P. J. Flory, *ibid.* **61**, 5366 (1974).
[3] (a) R. L. Jernigan and P. J. Flory, J. Chem. Phys. **50**, 4178 (1969); (b) **50**, 4185 (1969); (c) K. Nagai, *ibid.* **48**, 5646 (1968).
[4] B. Valeur and L. Monnerie, J. Polym. Sci. Polym. Phys. Ed. **14**, 11 (1976).
[5] P. D. Hyde, D. A. Waldow, M. D. Ediger, T. Kitano, and I. Koichi, Macromolecules **19**, 2533 (1986).
[6] T. A. Weber and E. Helfand, J. Phys. Chem. **87**, 2881 (1983).
[7] J. P. Jarry and L. Monnerie, J. Polym. Sci. Polym. Phys. Ed. **16**, 443 (1978).

[8]R. L. Jernigan, in *Dielectric Properties of Polymers*, edited by F. E. Karasz (Plenum, New York, 1972).
[9]I. Bahar and B. Erman, Macromolecules **20**, 1368 (1987).
[10]B. J. Berne and R. Pecora, *Dynamic Light Scattering* (Wiley, New York, 1976).
[11](a) P. G. de Gennes, *The Physics of Liquid Cristals* (Clarendon, London, 1974); (b) W. Maier, and A. Saupe, Z. Naturforsch. A **13**, 564 (1958); **14**, 882 (1959); **15**, 287 (1960).
[12]A. Abe, R. L. Jernigan, and P. J. Flory, J. Am. Chem. Soc. **88**, 631 (1966).
[13]H. A. Kramers, Physica **7**, 284 (1940).
[14]J. Skolnick and E. Helfand, J. Chem. Phys. **72**, 5489 (1980).
[15]B. Valeur, J. P. Jarry, F. Gény, and L. Monnerie, J. Polym. Sci. Polym. Phys. Ed. **13**, 667 (1975); **13**, 657 (1975).
[16]J. T. Bendler and R. Yaris, Macromolecules **11**, 670 (1978).
[17]J. Skolnick and R. Yaris, Macromolecules **15**, 1041 (1982).
[18]C. K. Hall and E. Helfand, J. Chem. Phys. **77**, 3275 (1982).
[19]J. Skolnick and R. Yaris, Macromolecules **15**, 1046 (1982).
[20]A. Abe, H. Furuya, and H. Toriumi, Macromolecules **17**, 684 (1984).
[21]K. A. Dill and P. J. Flory, Proc. Natl. Acad. Sci. USA **77**, 3115 (1980).
[22]K. A. Dill and P. J. Flory, Proc. Natl. Acad. Sci. USA **78**, 676 (1981).
[23]P. J. Flory and D. Y. Yoon, Nature **272**, 226 (1978).